Modification of a screen-printed carbon electrode with nanoporous gold by electrodeposition and dealloying of a gold-copper alloy

Nur Asyiqin Azman[1], Yusairie Mohd[1], Zainiharyati Mohd Zain[1], Lim Ying Chin[1*]

[1]Electrochemical Materials and Sensor (EMaS) Research Group, Faculty of Applied Sciences, Universiti Teknologi MARA, 40450 Shah Alam, Selangor, Malaysia.

ABSTRACT

In this study, a three-dimensional structure of nanoporous gold (NPG) was made by selectively corroding copper (Cu) from gold-copper (Au-Cu) alloys using a two-step electrochemical method. Given its large surface area and interconnected porous network, nanoporous gold is a suitable material for the advancement of electrochemical sensors. The screen-printed carbon electrode (SPCE) modified with nanoporous gold (NPG/SPCE) was fabricated by electrodepositing a gold-copper alloy from gold ion (Au^{3+}) and copper ion (Cu^{2+}) solution via cyclic voltammetry (CV) by scanning from -0.3 V to -0.8 V for 80 cycles. The copper is then removed via a dealloying process in 3M HNO_3 using the cyclic voltammogram (CV) method by scanning potential from 0 V to +1.0 V for 100 cycles at 100 mV/s. The morphology, elemental composition, and electrochemical active surface area (ECSA) of NPG/SPCE electrodes were characterized using FESEM, EDX, and CV analysis, respectively. The electrochemical performance of the NPG/SPCE was compared with bare SPCE in a 10 mM potassium ferrocyanide (K_4FeCN_6) solution using cyclic voltammetry. The morphological study using FESEM revealed that the NPG/SPCE had an average pore diameter of 53 nm. The quantification of elements using EDX shows that 84 % of the copper in the electrodeposited gold-copper alloy electrode was successfully removed by the dealloying process. The higher number of cycles during the dealloying process led to producing NPG with higher ECSA electrodes. The ECSA of NPG/SPCE is 12 times greater than that of bare or unmodified SPCE in an equivalent geometrical area. NPG/SPCE has a much better electron transfer surface than bare SPCE due to its high surface area and gold surface properties, making it a potential sensing material for biosensing applications.

Keywords: dealloying, electrodeposition, gold alloy, nanoporous gold, screen-printed electrode.

1. INTRODUCTION

Nanoporous gold (NPG) receives particular interest for its high active area, excellent conductivity, and biocompatibility to be applied to various applications such as electrochemical biosensors, energy conversion and storage systems and drug delivery devices [1]–[3]. The gold nanoporous structure can be acquired through the dealloying process of gold alloys, which eliminates more active elements from the Au alloy film. Briefly, during the dealloying process, the more active constituent of alloy film is selectively dissolved into the solution, leaving behind the three-dimensional interconnected porous structure of the more noble metal element. Alloys can be fabricated through vapor deposition, sputter deposition, or electrodeposition, whereas dealloying can take place in a very concentrated acid or by applying an electrochemical potential to dilute acids. [4]. Tuning the electrodeposition condition allows greater control of surface morphologies such as the thickness of the film, surface roughness, size, and shape of the

---

nanostructure. This electrodeposition method is simple to implement by controlling either applied potential and current, the number of scan cycles, or the scan rate. It is critical to understand that different metal elements have different potentials for the metal ion to undergo reduction. As a result, for both metal ions to be electrodeposited on a screen-printed carbon electrode, a range of potentials must be applied. Dealloying can be achieved electrochemically or through a chemical dealloying process in a highly corrosive solution. Chemical dealloying of gold-silver (Au-Ag) or gold-copper (Au-Cu) alloys in concentrated nitric acid with a molarity greater than 15 M is commonly used to create nanoporous gold (NPG) [5]–[7]. El Mel group used 70% nitric acid to dealloy Au-Cu film using a chemical dealloying process and required 5 hours for 100% of the Cu element to be dissolved [8]. However, when fabricating nanoporous gold (NPG) on screen-printed electrodes, highly corrosive solutions are not desirable. It is because the chemical dealloying method will cause the printed reference electrode and the counter electrode to detach from their ceramic substrate. Alternatively, NPG films can be produced by catalyzing the dealloying process with the electrochemical method in dilute acid solutions [5], [9]. However, this application requires a specific potential for selectively dissolving the more reactive element. The electrochemical dealloying approach allows a faster and more precise measure of the etching or dissolution process, lowers costs, and reduces corrosive waste compared with the chemical dealloying method. The electrodeposition and leaching conditions must be properly controlled to get the diameter, shape, and density of the nanopores (i.e., time, temperature, and concentration).

In this study, we focus on fabricating nanoporous gold structures using the electrochemical method, from alloying to dealloying on the screen-printed carbon electrode. The present work aims to highlight the use of the dealloying method that can produce a high electrochemical active surface area and a uniform, homogeneous coating that can be utilized in sensor applications. Earlier studies [10]–[16] employed the pulse electrochemical dealloying method on commercial gold alloys, where a specific potential was applied to the alloy for a set duration of time. However, this method is not suitable for use with screen-printed carbon electrodes (SPCE), as the printed silver reference electrode (RE) will oxidize when exposed to the Au-Cu alloy solution, leading to a shift in reduction potential due to a galvanic replacement reaction between silver metal and gold ions in the solution. Therefore, to integrate SPCE as the deposition and dealloying substrate, cyclic voltammetry was implied by applying a certain range of potential for electrodeposition and electrochemical dealloying. This process may aid in the optimization of the electrochemical condition to obtain a better morphological structure and improve the electrochemical performance of the NPG electrode. Dilute nitric acid was chosen as the etching solution for the dealloying process in order to avoid the silver (Ag) reference electrode from being oxidized. Field Emission Scanning Electron Microscopy (FESEM), Energy Dispersive X-Ray (EDX), and cyclic voltammetry analyses were employed to study the surface properties and electrochemical behavior of the Au-Cu alloy and NPG electrode.

2. MATERIAL AND METHODS

2.1 Materials and chemicals

A screen-printed carbon electrode (SPCE) with a carbon working electrode diameter of 0.11 cm^2, silver (Ag) as the reference electrode, and carbon as the counter electrode was purchased from Metrohm Malaysia Sdn. Bhd. Gold (III) chloride trihydrate >99.9 % ($HAuCl_4.3H_2O$) and potassium hexacyanoferrate (II) trihydrate (K_4FeCN_6) were purchased from Sigma-Aldrich, Germany. Potassium chloride >99.999 % (KCl) used as supporting electrolytes was purchased from Thermo Scientific, USA. Nitric acid (69.0–70.0 %) and sulphuric acid (96 %) were purchased from Fisher Scientific (M) Sdn Bhd.

2.2   Instruments

Electrochemical analyses, electrodeposition, and dealloying processes were performed on the DropSens Portable Potentiostat/Galvanostat/Impedance Analyzer (EIS) STAT-I 400s (Oviedo, Spain) electrochemical system interfaced with the DropView 8400 software. Morphological study of the NPG/SPCE electrode was obtained using a Field Emission Scanning Electron Microscope (FESEM, JEOL model JDM-7600F) operating at a voltage of 5 kV and interfaced with an Energy Dispersive X-Ray (EDX) spectrometer for elemental study.

2.3   Electrodeposition and dealloying of gold-copper (Au-Cu) alloy on SPCE

The gold nanoporous electrode was fabricated by coating a screen-printed carbon electrode with Au-Cu alloy and then dealloying the alloy electrode with HNO_3 solution to create a porous structure. Prior to the deposition process, cyclic voltammetry in a 2:8 mM Au-Cu alloy solution was carried out by scanning from +1 V to -1 V to find the optimum potential for deposition. After that, the Au-Cu alloy was electrodeposited on SPCE by cyclic voltammetry mode by scanning from -0.3 V to -0.8 V for 80 cycles at 100 mV/s in 2:8 mM Au-Cu alloy solution containing 1 M H_2SO_4, producing an Au-Cu/SPCE electrode. The deposition was cycled 80 times, which is equivalent to 15 minutes, as referred to [10], [17]. The Au-Cu/SPCE electrode was then de-alloyed via cyclic voltammetry for the removal of Cu from the alloy electrode, which then resulted in a porous structure. The dealloying potential range used was from 0 V to +1 V for 100 cycles at 100 mV/s in 3 M HNO_3. The effect of the number of scanning cycles during the dealloying process was investigated with respect to the NPG electrochemical performance. Finally, the electrodes were dried under a nitrogen stream.

2.4   Electrochemical measurements

All electrochemical measurements were performed using fabricated gold nanoporous (NPG/SPCE) (diameter 4 mm) with a built-in carbon auxiliary electrode and silver reference electrode. The cyclic voltammetry measurement was performed in 0.1 M KCl containing 10 mM K_4FeCN_6. By performing CV in 0.5 M H_2SO_4, the electrochemical active surface area (ECSA) and roughness factor of NPG were determined from the cathodic area of the voltammogram corresponding to gold oxide reduction to gold by applying potential from +0.2 V to +1.8 V at 100 mV/s.

3.   RESULTS AND DISCUSSION

3.1   Electrodeposition and Dealloying of Gold-Copper (Au-Cu) Alloy on SPCE

Prior to the electrodeposition of Au-Cu alloy on SPCE, a cyclic voltammogram of SPCE in a bath solution containing both ions (Au^{3+} and Cu^{2+}) was plotted to determine the optimal potential range for Au-Cu alloy deposition. Figure 1 shows the cathodic peak waves, ipc_1 and ipc_2, which appeared at +0.12 V and +0.02 V corresponding to the two successive reductions of gold as shown in equations (1) and (2), respectively, with both processes introducing chloride ions into the solution [17]. Meanwhile, further scanning to a more negative potential, two more cathodic peaks, ipc_3 and ipc_4 appeared at -0.44 V and -0.77 V corresponding to the reduction of copper as shown in equations (3) and (4), respectively [18].

$AuCl_4^- + 2\ e^- \rightarrow AuCl_2^- + 2\ Cl^-$ $\qquad\qquad$ (1)
$AuCl_2^- + 1\ e^- \rightarrow Au(0) + 2\ Cl^-$ $\qquad\qquad$ (2)
$Cu^{2+} + 1\ e^- \rightleftharpoons Cu^+$ $\qquad\qquad$ (3)
$Cu^+ + 1\ e^- \rightleftharpoons Cu(0)$ $\qquad\qquad$ (4)

On the reverse oxidative sweep, the anodic peaks at ipa$_1$ (-0.58 V) and ipa$_2$ (-0.41 V) exhibit reversibility of Cu(I/0) to two successive oxidation, reverse equation of equations (3) and (4). The two-step oxidation of Cl$^-$ at the gold surface is consistent with the other two oxidation processes observed at ipa$_3$ (+0.37 V) and ipa$_4$ (+0.52 V). Peak ipa$_3$ is attributed to the two-electron oxidation of chloride to trichloride, equation (5), whereas peak ipa$_4$ is attributed to the following one-electron oxidation, which releases chlorine gas, equation (6) [17].

$$3\ Cl^- \rightarrow Cl_3^- + 2\ e^- \tag{5}$$
$$2\ Cl_3^- \rightarrow 3\ Cl_2 + 2\ e^- \tag{6}$$
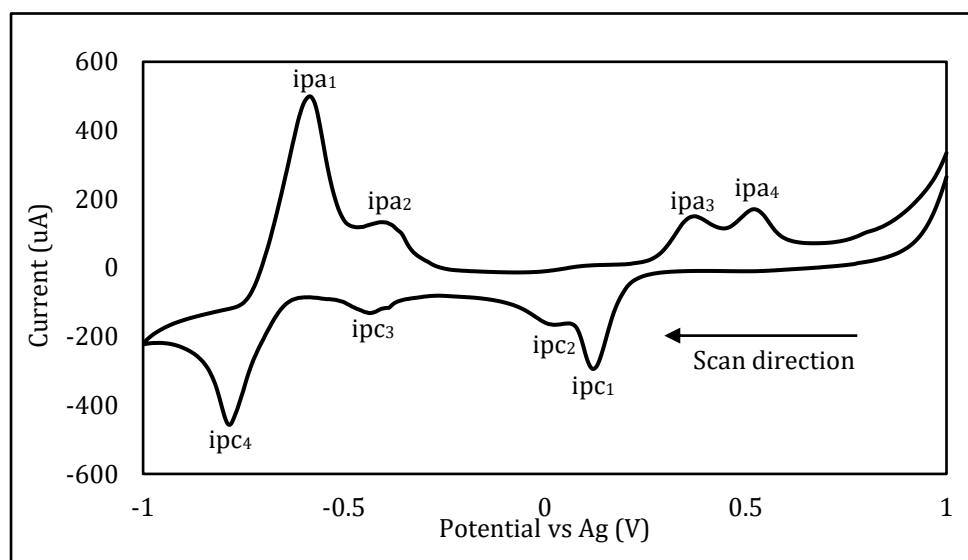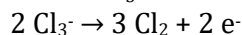
Figure 1. Cyclic voltammogram of SPCE in Au-Cu alloy solution + 0.1 M H$_2$SO$_4$ scanned at 100 mV/s

Since gold and copper have different standard reduction potentials, the reduction peak of both metal ions in the Au-Cu alloy solution is separated. For both elements to be deposited on the SPCE surface, a potential range between ipc$_1$ and ipc$_4$ was applied. Au-Cu alloy was electrodeposited by applying potential from -0.3 V to -0.8 V and back to -0.3 V. Figure 2 shows a cyclic voltammogram of the electrodeposition process of a gold-copper alloy on SPCE where the potential between -0.3 V and -0.8 V was cycled 80 times at 100 mV/s.

The carbon working electrode was observed to change from a black to a gold appearance after the electrodeposition process. The shifting of the reduction peak to a more positive potential from -0.48V in the first cycle to -0.32 V in the 80th cycle was observed in Figure 2, indicating that the electrodeposition of Au-Cu in the following scan took place on the Au-Cu alloy layer formed earlier after the first scan [15]. This is coherent with thermodynamics, which envisions that the nucleation of the subsequent layer of Au-Cu nanoparticles on the deposited Au-Cu alloy surface is easier than the nucleation of Au-Cu nanoparticles on SPCE. This is due to the deposition of any metal elements (i.e., Au, Cu, Ag) on the gold surface requiring less energy than deposition on the carbon surface. [19].
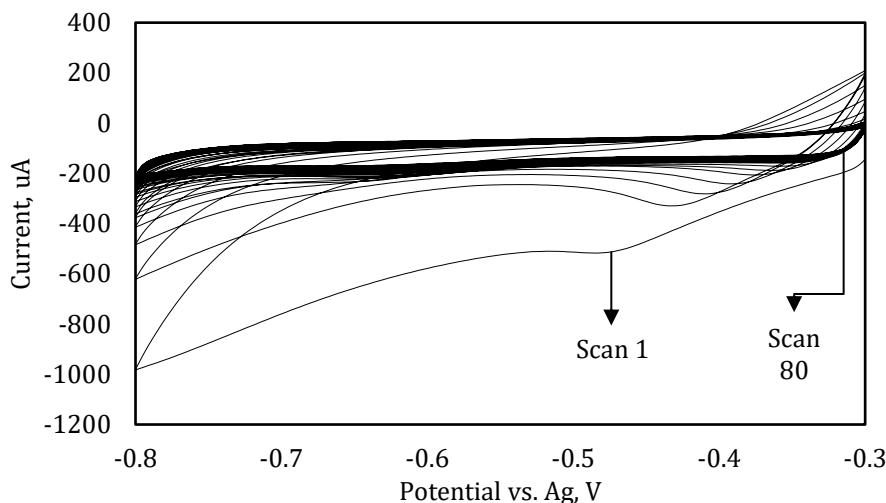
Figure 2. Cyclic voltammograms of the electrodeposition process of Au-Cu alloy on the SPCE surface for 80 cycles at 100 mV/s.

The deposition of the Au-Cu alloy is maintained at 80 cycles, so the electrochemical performance of NPG depends only on the dealloying cycle. Dealloying of gold-copper (Au-Cu) alloy was carried out in a 3 M HNO_3 solution by scanning potentials 0 V to +1 V for the different number of cycles in order to produce a porous gold structure, as shown by CV in Figure 3. During the dealloying process, less noble Cu is selectively dissolved, while Au will remain to form a nanoporous structure of gold. Applying positive potential will fasten the dealloying process, which causes Cu to leave the Au-Cu electrode surface, thus forming the nanoporous gold structure. The cyclic voltammograms of the dealloying process at the 1st cycle and 100th cycle are shown in Figure 3, where the oxidation peak of Cu at +0.15 V on the 1st cycle eventually disappeared in the 100th cycle scan. It was observed that at the 100th cycle of the CV, only oxidation and reduction peaks of Au appeared. This is because Cu(0) was completely removed from the alloy electrode surface.
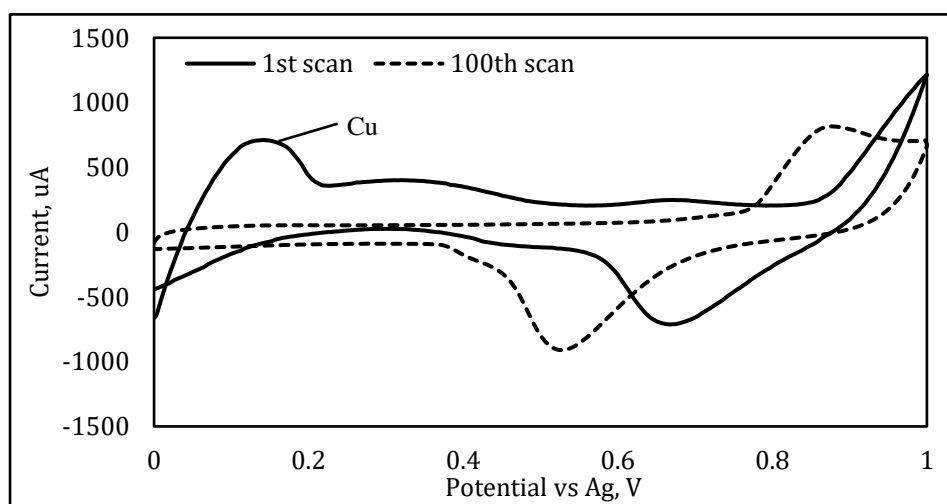
Figure 3. Cyclic voltammograms of the dealloying process of Au-Cu alloy in 3 M HNO_3 for 1st and 100th cycles at 100 mV/s

3.2 Cyclicvoltammogram (CV) response of $[Fe(CN)_6]^{4-/3-}$ ions on NPG/SPCE

The performance of the NPG/SPCE electrode was investigated by conducting cyclic voltammetry in 10 mM ferrocyanide ($[Fe(CN)_6]^{4-}$) + 0.1 M KCl. Since the deposition cycle of the Au-Cu alloy

was maintained at 80 cycles, the electrochemical performance of the NPG is solely dependent on the dealloying cycle (for example 10 cycles of the dealloying process is denoted as NPG-10). It was found that NPG-100 (ie: 100 cycles of dealloying process) has higher anodic/cathodic current peaks as compared to other NPG electrodes as summarized and depicted in Table 1 and Figure 4, respectively, An extended dealloying cycle leads to a higher quantity of copper dissolved into nitric acid, which enhances the surface area and improves the electrochemical performance of the NPG. However, there is no significant difference in redox current peak between NPG-100 and NPG-200 due to most of the copper had already been dissolved at 100 cycles.

Another notable difference is both oxidation and reduction peak potentials, E_{pa} and E_{pc} of $[Fe(CN)_6]^{4-/3-}$ on the NPG/SPCE electrode. The peak separation between E_{pa} and E_{pc} becomes smaller with an increasing number of dealloying cycles. NPG-100 has the lowest peak separation value (E_{pa} - E_{pc}) compared to others modified electrodes as summarised in Table 1. The electron-transfer kinetics of the electrode influence the redox peak separation values. Small redox peak separation implies that the electrode surface aids the electron transfer reaction of $[Fe(CN)_6]^{4-/3-}$ ions. The increase in E_{pa} - E_{pc}, on the other hand, was caused by the electrode surface undergoing a redox reaction with slow electron transfer [15], [20]. In comparison to the previous study, the NPG/SPCE of this study has obtained a 60 % lower peak separation value than Zakaria et al. (2021), who obtained +0.2 V for the average value of peak separation of the AuNP/GCE electrode. This is because the NPG/SPCE with a nanoporous structure provides more active surface area for a faster electron transfer reaction of $[Fe(CN)_6]^{4-/3-}$ ions to occur.
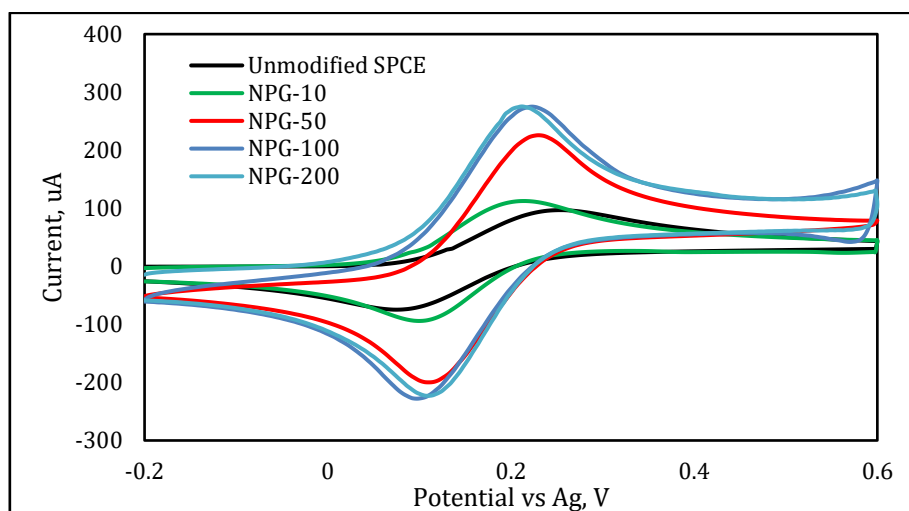
Figure 4. Cyclic Voltammograms of unmodified SPCE, NPG-10, NPG-50, NPG-100 and NPG-200 electrodes in 10 mM $K_4[Fe(CN)_6]$ + 0.1 M KCl solution

Table 1. A summary of the anodic, cathodic and peak separation values of unmodified SPCE and NPG electrodes

Electrode	E_{pa} (V)	E_{pc} (V)	E_{pa}-E_{pc} (V)	Anodic Current (I_{pa})	Cathodic Current (I_{pc})
Unmodified SPCE	0.252	0.064	0.188	81.102	-67.03
NPG-10	0.224	0.096	0.128	98.342	-98.933
NPG-50	0.232	0.110	0.122	211.425	-206.089
NPG-100	0.216	0.098	0.118	230.779	-229.874
NPG-200	0.220	0.101	0.119	223.978	-228.793

3.3 Surface characterization of Au-Co alloy and NPG electrode

FESEM provides one of the most informative techniques to study the surface morphology (i.e., size and shape) of the electrodeposited metal nanoparticles. FESEM analysis was used in this study to investigate the surface structural morphology of the electrodeposited Au-Cu alloy (Au/Cu/SPCE) and nanoporous Au electrode (NPG/SPCE).

The heterogeneous surface of bare SPCE (Figure 5a) contributes to the agglomeration of Au-Cu nanoparticles during the deposition process due to its stable nucleating surface already present [21]. Figures 5b shows the FESEM images of the Au-Cu alloy deposit at a magnification of 5 K and 100 K after the deposition process. Notably, the Au-Cu alloy deposits comprise a variety of quasi-spherical and facetted nanoparticles with particle size around 500 nm. Agglomeration of nanoparticles also occurs due to the nanoparticles tending to grow on the previously formed Au-Cu alloy nanoparticles, which is consistent with the shifting of the cathodic peak as shown earlier by CV in Figure 2. After the dealloying process, the interconnected nanoporous structure was formed, as shown in Figures 5c at 5K and 100K magnification. Inset Figure 5c depicts an interconnected porous structure aggregated by Au particles that join together with around 50 nm pores in diameter.

Au-Cu alloy and NPG electrodes were subjected to EDX analysis to investigate the presence of their elemental compositions. From Figure 6a, the Au-Cu alloy surface exhibited two main peaks related to gold and copper, which account for approximately 79 % of surface compositions as summarized in Table 2. The presence of carbon on both electrode surfaces might be due to the inhomogeneous deposition process that does not cover the entire bare carbon substrate. Figure 6b displays an obvious decrease in the weight percent of copper, whereas the composition of carbon and gold peaks was maintained after the dealloying process.

On the other hand, the NPG surface was rich in gold, with 73.1 % and only 0.86 % of copper detected on the carbon surface (i.e., 85 % Cu removal), indicating a successful dealloying process. The remaining 15 % of Cu was unable to dissolve during the dealloying process due to the agglomeration of the Au-Cu alloy, which hindered the HNO_3 from reaching the underneath Cu, whereas another 25.91 % accounted for carbon, which suggested that the gold nanostructures do not cover the bare carbon surface completely. Thus, it is recommended to increase the time of deposition in order to completely cover the entire SPCE surface with gold alloy.
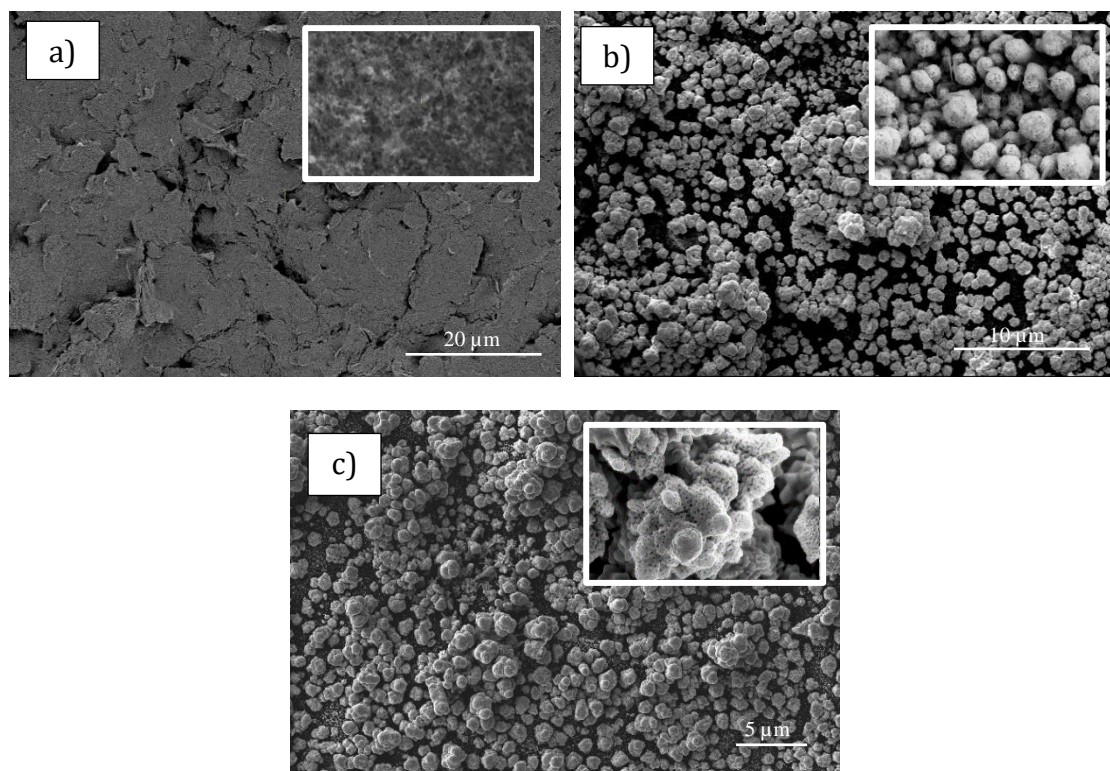
Figure 5. FESEM images of a) bare SPCE, b) Au-Cu/SPCE and c) nanoporous Au electrode at 5K. (Inset images at 100K magnification, respectively)
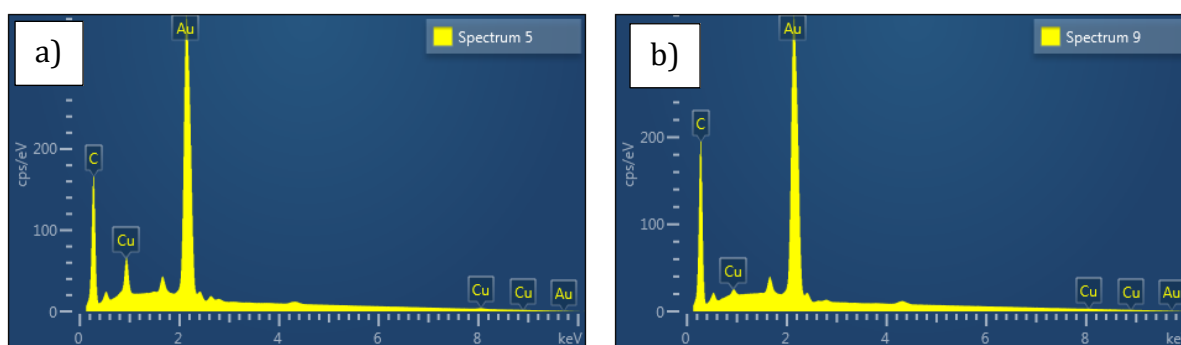
Figure 6. Energy Dispersive X-ray spectroscopy (EDX) spectra of (a) Au-Cu alloy and (b) NPG electrode.

Table 2. Elemental composition of the Au-Cu alloy and NPG electrode

Electrode	Elemental composition (wt.%)		
	Gold (Au)	Copper (Cu)	Carbon (C)
Au-Cu Alloy	73.07	5.41	21.52
NPG	73.23	0.86	25.91

3.4 Electrochemical active surface area and roughness factor of NPG/SPCE

The surface area is an important concern, as it will enhance the electrocatalytic activity of the modified SPCE electrode. A cyclic voltammogram of NPG/SPCE in a 0.5 M H_2SO_4 solution was recorded to investigate the electrochemical active surface area (ECSA) of the prepared NPG/SPCE, as shown in Figure 6. From the voltammogram, a small increment of anodic current at +1.1 V was observed on the forward scan, corresponding to the electrochemical oxidation of gold, and while a cathodic peak appeared at +0.5 V due to the reduction of gold oxide to gold on the reverse scan. The electrochemical active surface area (ECSA) and roughness factor (ρ) of the NPG/SPCE electrode were calculated using equations 7-9 by integrating the gold oxide reduction peaks in the negative-going scan from +0.7 V to +0.35 V. The electrode was assumed to be covered by one monolayer of adsorbed oxygen with a transferred charge of 868 μC cm^{-2} [22].

$$\text{charge}(Q) = \frac{\text{integrated area under reduction peak}}{\text{scan rate of CV}} \tag{7}$$

$$\text{Electrochemical active surface area (ECSA)} = \frac{Q}{Q_{\text{theoretical}}} \tag{8}$$

$$\text{Roughness factor } (\rho) = \frac{\text{ECSA}}{A_{\text{geo}}} \tag{9}$$

where Q is the Faradaic charge passed up during the experiment, $Q_{\text{theoretical}}$ is the theoretical charge density of Au given in the literature as 390 μC cm^{-2} [15] and A_{geo} is the geometrical area of the working electrode of SPCE, which is 0.11 cm^2. The ECSA and ρ of the NPG /SPCE are 1.36 cm^2 and 12.36, respectively. Assuming that the ECSA of bare SPCE is similar to its geometrical area, the modification of SPCE with NPG is able to increase the ECSA by 12 times. The data obtained indicate that the NPG/SPCE has a larger and rougher surface, which enhances the electrochemical performance of the electrode as can be seen in Table 3. This is consistent with the porous structure on NPG/SPCE electrode, which provides more surface area for electron transfer mechanism reactions to occur as compared to the particle-like structure. Greater ECSA can result in faster electron transfer, more efficient mass transfer, and significantly improved electrochemical output [23].
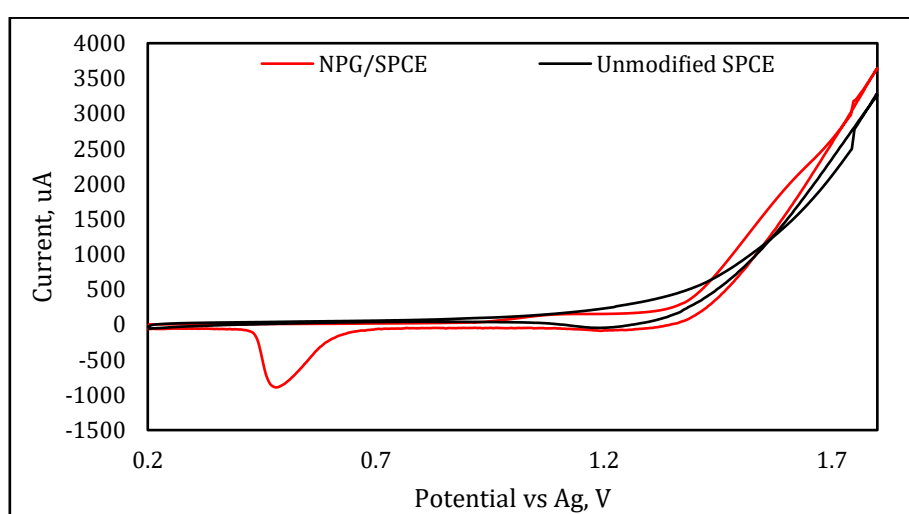
Figure 7. Cyclic voltammogram of NPG/SPCE and unmodified SPCE recorded in 0.5 M H_2SO_4 at 100 mV/s.

Table 2 Detailed comparison of the ECSA, roughness factor and pore size of gold nanostructures using various electrodes.

Method	Electrode	ESCA (cm²)	Roughness factor (ρ)	Pore size (nm)	Ref.
Electrodeposition	AuNP	0.085	-	-	[10]
		0.09	-	-	[15]
Anodization	NPG	0.216	4.7	10 to 50	[24]
		-	6	-	[25]
		0.69	-	60 to 130	[14]
Chemical dealloying	NPG	-	-	10 to 75	[8]
		-	7.65	12.8	[12]
Dropcast	CuO/Co$_3$O$_4$@MWCNTs	0.115	-	-	[26]
Electrochemical dealloying	NP-Ni	-	-	100 to 200	[11]
	NP-Pd	-	-	30 to 60	[13]
	NPG	1.36	12.36	40	This work

4. CONCLUSION

In conclusion, a two-step approach to the synthesis process for the modification of SPCE with a nanoporous gold structure (NPG/SPCE) was successfully developed. This approach is based on the electrodeposition of Au-Cu by cyclic voltammetry followed by the removal of Cu using a dealloying process in nitric acid. Although not often used, CV is proved to be an efficient deposition mode for electrodepositing Au-Cu nanoparticles on SPCE and the dealloying process of the Au-Cu alloy electrode is done to form a nanoporous structure of gold. The pore diameter of the porous structure of the gold deposit was around 50 nm. This porous structure of gold with high ECSA and surface roughness has significantly enhanced the electron-transfer kinetics of $[Fe(CN)_6]^{4-/3-}$ redox reactions, as shown by the small peak separation (E_{pa} - E_{pc}) value. It was found that the number of scanning cycles for the dealloying process has significantly affected the formation of NPG/SPCE. The excellent electrochemical performance of the modified SPCE electrode is associated with the gold nanoporous structure and the superior electrical conductivity of the gold element. The findings presented here will be valuable in understanding the growth mechanisms of gold alloy nanoparticles on the SPCE surface and the fabrication of nanoporous gold using a two-step process (i.e., deposition of gold alloy and dealloying process of the alloy) for use in electrochemical sensor technologies.

REFERENCES

[1]	K. Rong, L. Huang, H. Zhang, J. Zhai, Y. Fang, and S. Dong, "Electrochemical fabrication of nanoporous gold electrodes in a deep eutectic solvent for electrochemical detections," *Chemical Communications*, vol. 54, no. 64, pp. 8853–8856, 2018, doi: 10.1039/c8cc04454f.

[2]   J. Zhang and C. M. Li, "Nanoporous metals: fabrication strategies and advanced electrochemical applications in catalysis, sensing and energy systems," *Chemical Society Review*, vol. 41, no. 21, pp. 7016–7031, 2012, doi: 10.1039/C2CS35210A.

[3]   T. M. Martin, D. B. Robinson, and R. J. Narayan, "7 - Nanoporous gold for biomedical applications: structure, properties and applications**Note: This chapter is a reprint of Chapter 4 'Nanoporous gold for biomedical applications: structure, properties and applications' by T. M. Martin, D. B. Robinson and R. J. Narayan, originally published in Nanomedicine: Technologies and applications, ed. T. J. Webster, Woodhead Publishing Limited, 2012, ISBN: 978-0-85709-233-5.," in *Precious Metals for Biomedical Applications*, N. Baltzer and T. Copponnex, Eds. Woodhead Publishing, 2014, pp. 148–162. doi: https://doi.org/10.1533/9780857099051.2.148.

[4]   J.-F. Huang and I.-W. Sun, "Fabrication and surface functionalization of nanoporous gold by electrochemical alloying/dealloying of Au–Zn in an ionic liquid, and the self-assembly of L-Cysteine monolayers," *Advanced Functional Material*, vol. 15, no. 6, pp. 989–994, 2005, doi: https://doi.org/10.1002/adfm.200400382.

[5]   J. Fu, Z. Deng, and E. Detsi, "Nanoporous Gold Formation by Free Corrosion Dealloying of Gold-Silver Alloys in Nonoxidizing Acids Driven by Catalytic Oxygen Reduction Reaction," *JOM*, vol. 71, no. 4, pp. 1581–1589, Apr. 2019, doi: 10.1007/s11837-019-03383-1.

[6]   E. Detsi, M. Salverda, P. R. Onck, and J. T. M. de Hosson, "On the localized surface plasmon resonance modes in nanoporous gold films," *J Appl Phys*, vol. 115, no. 4, Jan. 2014, doi: 10.1063/1.4862440.

[7]   D. Jalas, R. Canchi, A. Y. Petrov, S. Lang, L. Shao, J. Weissmüller and M. Eich, "Effective medium model for the spectral properties of nanoporous gold in the visible," *Applied Physic Letter*, vol. 105, no. 24, p. 241906, Dec. 2014, doi: 10.1063/1.4904714.

[8]   A.-A. el Mel *et al.*, "Unusual Dealloying Effect in Gold/Copper Alloy Thin Films: The Role of Defects and Column Boundaries in the Formation of Nanoporous Gold," *ACS Applied Material Interfaces*, vol. 7, no. 4, pp. 2310–2321, Feb. 2015, doi: 10.1021/am5065816.

[9]   G. Ruffato, F. Romanato, D. Garoli, and S. Cattarin, "Nanoporous gold plasmonic structures for sensing applications," *Optics Express*, vol. 19, no. 14, pp. 13164–13170, Jul. 2011, doi: 10.1364/OE.19.013164.

[10]   C. Hou, Q. Luo, Y. He, and H. Zhang, "Potentiostatic electrodeposition of gold nanoparticles: variation of electrocatalytic activity toward four targets," *Journal of Applied Electrochemistry*, vol. 51, no. 12, pp. 1721–1730, 2021, doi: 10.1007/s10800-021-01604-7.

[11]   L. Sun, C. L. Chien, and P. C. Searson, "Fabrication of nanoporous nickel by electrochemical dealloying," *Chemistry of Materials*, vol. 16, no. 16, pp. 3125–3129, Aug. 2004, doi: 10.1021/cm0497881.

[12]   F. Zhao, J. Zeng, M. M. P. Arnob, P. Sun, J. Qi, P. Motwani, M. Gheewala, C. H. Li, A. Paterson, U. Strych, and B. Raja, "Monolithic NPG nanoparticles with large surface area, tunable plasmonics, and high-density internal hot-spots," *Nanoscale*, vol. 6, no. 14, pp. 8199–8207, Jul. 2014, doi: 10.1039/c4nr01645a.

[13]   J. Yu, Y. Ding, C. Xu, A. Inoue, T. Sakurai, and M. Chen, "Nanoporous metals by dealloying multicomponent metallic glasses," *Chemistry of Materials*, vol. 20, no. 14, pp. 4548–4550, Jul. 2008, doi: 10.1021/cm8009644.

[14]   L. E. Ahangar and M. A. Mehrgardi, "Nanoporous gold electrode as a platform for the construction of an electrochemical DNA hybridization biosensor," *Biosensors & Bioelectronics*, vol. 38, no. 1, pp. 252–257, Oct. 2012, doi: 10.1016/j.bios.2012.05.040.

[15] N. D. Zakaria, M. H. Omar, N. N. Ahmad Kamal, K. Abdul Razak, T. Sönmez, V. Balakrishnan and H. H. Hamzah, "Effect of supporting background electrolytes on the nanostructure morphologies and electrochemical behaviors of electrodeposited gold nanoparticles on glassy carbon electrode surfaces," *ACS Omega*, vol. 6, no. 38, pp. 24419–24431, Sep. 2021, doi: 10.1021/acsomega.1c02670.

[16] J. M. Doña Rodríguez, J. A. Herrera Melián, and J. Pérez Peña, "Determination of the real surface area of Pt electrodes by hydrogen adsorption using cyclic voltammetry," *Journal of Chemical Education*, vol. 77, no. 9, p. 1195, Sep. 2000, doi: 10.1021/ed077p1195.

[17] L. Aldous, D. S. Silvester, C. Villgran, W. R. Pitner, R. G. Compton, M. C. Lagunas and C. Hardacre, "Electrochemical studies of gold and chloride in ionic liquids," *New Journal of Chemistry*, vol. 30, no. 11, pp. 1576–1583, 2006, doi: 10.1039/B609261F.

[18] S. Malini, K. Raj, and A. Reddy, "Cyclic Voltametric Studies of the Interaction of Rizatriptan Benzoate with Copper in Aqueous Solution," *International Research Journal of Pharmacy*, vol. 8, pp. 117–121, Nov. 2017, doi: 10.7897/2230-8407.0810192.

[19] T. Hezard, K. Fajerwerg, D. Evrard, V. Collire, P. Behra, and P. Gros, "Gold nanoparticles electrodeposited on glassy carbon using cyclic voltammetry: Application to Hg(II) trace analysis," *Journal of Electroanalytical Chemistry*, vol. 664, pp. 46–52, Jan. 2012, doi: 10.1016/j.jelechem.2011.10.014.

[20] A. Maringa and T. Nyokong, "The influence of gold nanoparticles on the electroactivity of nickel tetrasulfonated phthalocyanine," *Journal of Porphyrins and Phthalocyanines*, vol. 18, no. 08n09, pp. 642–651, Aug. 2014, doi: 10.1142/S1088424614500333.

[21] N. T. K. Thanh, N. Maclean, and S. Mahiddine, "Mechanisms of nucleation and growth of nanoparticles in solution," *Chemical Reviews*, vol. 114, no. 15. American Chemical Society, pp. 7610–7630, Aug. 13, 2014. doi: 10.1021/cr400544s.

[22] S. Cherevko, A. A. Topalov, A. R. Zeradjanin, I. Katsounaros, and K. J. J. Mayrhofer, "Gold dissolution: Towards understanding of noble metal corrosion," *RSC Adv*, vol. 3, no. 37, pp. 16516–16527, Oct. 2013, doi: 10.1039/c3ra42684j.

[23] J. Yoon, B. M. Conley, M. Shin, J. H. Choi, C. K. Bektas, J. W. Choi and K. B. Lee, "Ultrasensitive electrochemical detection of mutated viral RNAs with single-nucleotide resolution using a nanoporous electrode array (NPEA)," *ACS Nano*, vol. 16, no. 4, pp. 5764–5777, Apr. 2022, doi: 10.1021/acsnano.1c10824.

[24] K. Rong, L. Huang, H. Zhang, J. Zhai, Y. Fang, and S. Dong, "Electrochemical fabrication of nanoporous gold electrodes in a deep eutectic solvent for electrochemical detections," *Chemical Communications*, vol. 54, no. 64, pp. 8853–8856, 2018, doi: 10.1039/C8CC04454F.

[25] Y. Mie, S. Katagai, and M. Ikegami, "Electrochemical oxidation of monosaccharides at nanoporous gold with controlled atomic surface orientation and non-enzymatic galactose sensing," *Sensors (Switzerland)*, vol. 20, no. 19, pp. 1–14, Oct. 2020, doi: 10.3390/s20195632.

[26] H. S. Magar, R. Y. A. Hassan, and M. N. Abbas, "Non-enzymatic disposable electrochemical sensors based on CuO/Co$_3$O$_4$@MWCNTs nanocomposite modified screen-printed electrode for the direct determination of urea," *Scientific Reports*, vol. 13, no. 1, p. 2034, Dec. 2023, doi: 10.1038/s41598-023-28930-4.